# Preferred orientation of ferromagnetic phases in rock-forming minerals: Insights from magnetic anisotropy of single crystals

e-mail: ann.hirt@erdw.ethz.ch

Keywords: magnetic anisotropy, ferromagnetic inclusions, ferromagnetic exsolutions, olivine, pyroxene, amphibole, feldspar, carbonate minerals, phyllosilicate minerals

**Abstract:** In the early days of paleomagnetism, David Strangway was interested in understanding why igneous rocks are faithful recorders of the Earth's magnetic field. He recognized that ferromagnetic (s.l.) grains that could be discerned by optical microscopy were too large to carry a stable remanent magnetization, and speculated whether fine-grained, ferromagnetic (s.l.) inclusions or exsolutions in silicate minerals are responsible. When these inclusions or exsolutions are randomly oriented, or the silicate hosts are randomly oriented in a rock, they can be a good recorder of the field. If these minerals, however, show an alignment within the silicate host, and the host is preferentially aligned due to flow structures or deformation, then the paleomagnetic direction and paleointensity could be biased. We examine the magnetic anisotropy arising from the ferromagnetic (s.l.) phases in silicate-host minerals. Single crystals of phyllosilicate, clinopyroxene and calcite show most consistent ferrimagnetic fabric with relation to the minerals' crystallographic axes, whereas olivine and feldspar display only a weak relationship. No discernable relationship is found between the ferrimagnetic anisotropy and crystallographic axes for amphibole minerals. Our results have implications when single crystals are being used for either studies of field direction or paleointensity or in cases where silicate minerals have a preferential orientation. Phyllosilicate minerals and pyroxene should be screened for significant magnetic anisotropy.

## Introduction

Some of the early research that David Strangway conducted was focused on understanding why volcanic rocks are good recorders of the Earth's magnetic field (Larson et al. 1969; Strangway et al. 1968). The formation of iron oxides, which serve as recorders for the Earth's magnetic field, during cooling of a magma was demonstrated by Buddington and Lindsley (1964) and Carmichael and Nicholls (1967), who investigated the role of oxygen fugacity in their formation. In studies on igneous rocks, Strangway and his collaborators noted that opaque grains, which were found in igneous rocks, were too large to carry stable remanent magnetization, i.e., be in the range of single domain. High temperature exsolution of titanomagnetite, however, led to the development of ilmenite lamellae together with magnetite. Exsolution reduces the effective particle size to the single domain range and results in an elongated shape of magnetite, which has high coercivity. Therefore, the high magnetic stability in the volcanic rocks was attributed to titanomagnetite grains that had undergone exsolution.

Strangway (1960) proposed also an alternative explanation for the high magnetic stability in igneous rocks, in which fine ferromagnetic (s.l.) minerals that are located within paramagnetic minerals, e.g., olivine, pyroxene, mica or feldspar, carry the stable magnetization. Ferromagnetic (s.l.) crystals can either exsolve within the paramagnetic host silicate during cooling, or become trapped during the formation of the silicate phase. The former are termed exsolutions, and form along distinct crystallographic directions or planes. The orientation of the latter is not constrained by the silicate crystal structure, and they are called inclusions. The term inclusion is also sometimes used as a generic term for both oriented exsolutions and unoriented inclusions. We will refer to ferromagnetic (s.l.) phases with a preferred orientation with respect to the silicate crystal structure as exsolutions, and use the term inclusions for randomly oriented phases incorporated during

crystal growth, or when it is not clear whether a ferromagnetic phase is an exsolution or inclusion. Strangway (1960) postulated that magnetite exsolutions, which formed within olivine and pyroxene crystals in diabase dikes of Precambrian age during late stage hydrothermal alteration, carry the stable remanent magnetization. Later investigations by other groups demonstrated that exsolutions can be responsible for primary magnetization in a rock (e.g., Hargraves and Young 1969; Strangway 1960; Tarduno et al. 2006; Wu et al. 1974). The remanent magnetization of exsolved phases is especially stable over geologic time because they are protected against chemical alteration. Wu et al. (1974) conducted the first study in which single silicate host grains with ferromagnetic (s.l.) exsolutions were oriented and demagnetized in order to obtain the direction of the paleofield. They found cloudy feldspars contained fine grains of magnetite that carry a stable magnetization, but biotite and hornblende grains contained larger magnetite particles, whose magnetization was unstable. Later studies also found that the ferromagnetic (s.l.) exsolutions in plagioclase were more likely to fall into the single-domain size range than exsolutions in olivine, pyroxene, biotite and hornblende (Cottrell and Tarduno 1999; Dunlop et al. 2006). Bono and Tarduno (2015) used exsolutions of single domain magnetite in feldspar as a stable recorder of the Earth's magnetic field in the Ediacaran. Buchan (1979), however, who separated oriented aggregates of light and dark minerals from the Bark Lake diorite, found that feldspar carried an unstable magnetization and biotite and hornblende were more likely to carry a more stable magnetization. Tarduno et al. (2006) provides a concise overview of early petrological, paleomagnetic and rock magnetic studies on these inclusions.

An important aspect when using single crystals for determination of paleomagnetic directions or paleointensities, is whether these show a preferential alignment due to exsolution along specific crystallographic directions. The first study to note the preferred orientation of

magnetite within pyroxene was Bown and Gay (1959), who identified two preferential orientations of magnetite exsolution, which are named "Z" and "X" exsolutions. Later studies also noted a preferred alignment in both pyroxene and amphiboles (Doukhan et al., 1990; Feinberg et al., 2004; Fleet et al., 1980), Clinopyroxenes show inclusions close to the crystallographic $[001]_{cpx}$ direction, Z inclusions, and the crystallographic $[100]_{cpx}$ direction, X direction. Augite crystals have $[\mathbf{1}10]_{mt}//[010]_{aug}$, $[111]_{mt}//(100)_{aug}$, $[\mathbf{11}2]_{mt}//[001]_{aug}$ with the magnetite lattice rotated 0.4° clockwise with respect to $[010]_{aug}$ for the "Z"-orientation, and $[\mathbf{1}10]_{mt}//[010]_{aug}$, $[\mathbf{11}1]_{mt}//(\mathbf{1}01)_{aug}$, $[112]_{mt}//[101]_{aug}$ with the magnetite lattice rotated 1.9° anticlockwise with respect to $[010]_{aug}$ for the "X"-orientation (Fleet et al., 1980). The exact angular rotation of the magnetite lattice in the case of pyroxene and amphibole will be dependent on the exsolution temperature (Fleet et al., 1980), but differences are small and will not affect the anisotropy tensor significantly.

Normally host silicates will be randomly distributed in a rock, which would mean that even if the exsolved magnetite is along preferred crystallographic directions within the silicate host, they would still be faithful recorders of the Earth's magnetic field. If the silicate hosts, however, show a crystallographic preferred orientation, then the magnetization of the exsolved magnetite could be biased to a preferred direction, as suggested by Cottrell and Tarduno (1999). For the past fifteen years, we have been interested in determining the intrinsic anisotropy of magnetic susceptibility in common rock forming minerals (Biedermann et al. 2014a, b; 2015a, b;. 2016; Martín-Hernández and Hirt 2003; Schmidt et al. 2006; 2007a). These minerals are diamagnetic or paramagnetic, and their intrinsic anisotropies have been determined using high-field torque magnetometry (Bergmüller et al. 1994), in order to isolate only the anisotropy arising from diamagnetism or paramagnetism (Martín-Hernández and Hirt 2001; 2004; Schmidt et al. 2007b). The method also isolates the ferromagnetic (s.l.) anisotropy arising from any low-coercivity

ferrimagnetic or high-coercivity antiferromagnetic phases within the host crystal. In this study, we report on the anisotropy of magnetic susceptibility (AMS) due to ferrimagnetic exsolutions in minerals to evaluate if there is a preferred orientation related to the crystal structure and composition of the host silicate. The high-field torsion magnetometer will only isolate a ferrimagnetic contribution if it is anisotropic. Inclusions that are randomly oriented will not contribute to the anisotropy, and thus not display any torque signal. Ferrimagnetic exsolutions were found mostly in phyllosilicate minerals, olivine, pyroxenes, amphiboles and feldspar. Some amphibole and feldspar crystals contain a high-coercivity phase, e.g. hematite, in addition to the ferrimagnetic inclusions. Carbonate minerals had little to no ferromagnetic (s.l.) phases within the crystals in general, but magnetite and hematite were found in several crystals. Rock magnetic methods were applied to aid in identification of the ferromagnetic (s.l.) inclusions.

## Samples and Methods

Samples were in the form of single crystals and were obtained from several sources, including the ETH mineral collection, the Natural History Museum Basel, Ward's Science (USA), Siber + Siber (Switzerland), Swiss Gemmological Society or from field work. It should be noted that crystals were chosen to cover the range of their silicate chemistry and may not represent the full range of exsolution orientations and aspect ratios, which may additionally depend on the crystal's cooling history. The crystals were oriented based on their crystal habit in the case of phyllosilicates, and calcite, or Laue X-ray diffraction for olivine, pyroxene, amphibole, and feldspar crystals. X-ray diffraction was carried out at the Laboratory of Crystallography, ETH Zürich. Orient Express 3.4, a crystal orientation software, was used to process the Laue images. Further details on the samples can be found in publications that report on the paramagnetic AMS

of the crystals (Biedermann et al. 2014 b; 2015a, b; 2016; Martín-Hernández and Hirt 2003; Schmidt et al. 2006; 2007a).

Acquisition of isothermal remanent magnetization (IRM) and magnetization curves were used to help identify ferromagnetic (s.l.) phases in the crystals. IRM acquisition curves were either obtained on a Princeton Measurements Corporation (PMC) magnetometer or by applying the IRM with an ASC impulse magnetizer (Model IM-10-30) and subsequently measuring the IRM on a 3-axis 2G Enterprises rock magnetometer. Magnetization curves were measured with a PMC vibrating sample magnetometer or alternating gradient magnetometer. High-field torque magnetometry was used to isolate the anisotropy arising from ferrimagnetic exsolutions in the crystals. The torque response of the samples was measured in three mutually perpendicular planes, by rotating the sample with 15° to 30° increments in at least four fields between 700 mT to 1800 mT. Isolation of the paramagnetic and ferrimagnetic AMS was obtained using methods described in Martín-Hernández and Hirt (2001). It should be noted that magnetic anisotropy is described by a symmetric second-order tensor, with its principal eigenvalues $k_1 \geq k_2 \geq k_3$. A torsion magnetometer, however, only defines the deviatoric tensor, i.e., deviations from a sphere whose diameter is the average susceptibility ($k_{avg}$). Therefore, in this paper the term $k_i$ for i = 1 to 3, is actually $k_i - k_{avg}$, which means that $k_1 + k_2 + k_3 = 0$. The shape of the anisotropy ellipsoid can be described by the U-factor (Jelinek 1981), which can take on a value between +1 for a rotationally oblate ellipsoid and -1 for a rotationally prolate ellipsoid, and the degree of anisotropy by the deviatoric susceptibility k' (Jelínek 1984), where

$$U = \frac{2k_2 - k_1 - k_3}{k_1 - k_3}$$

and $$k' = \sqrt{\left[(k_1 - k_{avg})^2 + (k_2 - k_{avg})^2 + (k_3 - k_{avg})^2\right]/3}$$

or

148 $\sqrt{[(k_1)^2 + (k_2)^2 + (k_3)^2]/3}$ for the deviatoric tensor

149

150 ## Results

151 **Phyllosilicate Crystals**

152 From the original studies of Martín-Hernández and Hirt (2003) and Biedermann et al. (2014a)
153 a total of five biotite, eleven phlogopite, five muscovite and five chlorite crystals were evaluated.
154 The biotite, muscovite and chlorite crystals all showed a ferrimagnetic component to the AMS,
155 but only one phlogopite had a significant ferrimagnetic component (Table S1). Most of these
156 crystals display a paramagnetic magnetization curve, although some crystals have a closed loop,
157 which is weakly defined after subtracting the paramagnetic slope (cf., Martín-Hernández and Hirt,
158 2003). All samples, except one muscovite crystal (Mu4), however, show the aquisition of an IRM.
159 The coercivity of remanence ($B_{CR}$) is between 12 mT and 50 mT, and the IRM is saturated by 200
160 mT, which inidcates the presence of low coercivity minerals (Fig. 1a).

161 The paramagnetic component to the AMS of all crystals have $k_3$ within 9° from the pole to
162 the basal plane, i.e., (001) (Martín-Hernández and Hirt, 2003), which indicates that the magnetic
163 fabric is controlled by the distribution of iron in the silicate sheet structure. The ferrimagnetic
164 component to the AMS has $k_3$ axes well grouped for all crystals except phlogopite, but canted by
165 an average of 37° ± 8° away from (001) and towards the basal plane (Fig. 1b, c, Table S). Note
166 that the [100] and [010] axes were not oriented; however, individual samples were cut from larger
167 crystals of bioite and muscovite and have therefore similar orientations with respect to each other.
168 The consistent orientation of the ferrimagnetic $k_3$ axes may indicate that their shape and orientation
169 is controlled by the silicate lattice, e.g. due to epitaxial growth. The shape of the ferrimagnetic
170 AMS ellispoid is oblate, except for the inclusions in phlogopite, whose AMS is prolate; the degree

of anisotropy is very weak for all crystals. Note that the exchange of the $k_2$ and $k_3$ axes in phlogopite may be due to its relatively strong prolate shape.

**Olivine Crystals**

Biedermann et al. (2014b) examined the AMS on 35 natural olivine, single crystals, whereby 34 of the crystals have a signifcant ferrimagnetic component to the high-field AMS (Table S2). Crystals often showed an open hysteresis loop after subtraction of the paramagnetic slope. The IRM of all crystals is saturated by 200 mT and $B_{CR}$ is between 12 mT to 37 mT, which shows that only low coercivity minerals are found as ferromagnetic (s.l.) phases (Fig. 2a).

The orientation of the principal axes of the paramagnetic susceptibility is dependent on the iron content in the olivine structure. Pure forsterite cystals with < 1 wt % FeO appear to be isotropic. All other crystlals have $k_1$ subparallel to [001], but $k_3$ is along [100] for forsterite crystals with 3–5 wt % FeO, and along [010] for crystals with 6–10 wt % FeO and weathered crystals with 16-18 wt % FeO.

The ferrimagnetic contribution to the high-field AMS can vary greatly and is between 4% to 87%. (Table S2). Ferrimagnetic directions do not show any strong preference in orientation with respect to the olivine lattice; however, $k_1$ and $k_3$ are concentrated at ca. 45° to [001], and $k_2$ tend to lie in the (001) plane. The shape of the AMS ellipsoid for the ferrimagnetic component is variable and can be oblate or prolate, and the degree of anisotropy is very low in all crystals except the crystal Ol14, which has the strongest ferrimagnetic component (Table S2).

**Pyroxene Crystals**

A total of 65 single crystals were used in the study of Biedermann et al. (2015b) in their study of the AMS of clinopyroxene and orthopyroxene. From the clinopyroxene crystals, 24 augite and one diopside carry a ferrimagnetic anisotropy, and hypersthene is the only orthopyroxene sample with a significant ferrimagnetic AMS. Enstatite, most diopside crystals, aegirine, and spodumene do not display a significant ferrimagnetic component of anisotropy. IRM acquistion shows that the crystals are saturated by 200 mT for most samples, only T13 is not saturated until 1000 mT (Fig. 3a). $B_{CR}$ is beween 12 mT and 46 mT, indicating a low coercivity phase, which is most likely magnetite.

The paramagnetic AMS was found to be related to crystalline structure and iron content. For diopside and augite, the $k_2$ axis is subparallel to [010] of the crystal, and $k_1$ and $k_3$ lie in a plane containing the [100] and [001] axes. For aegerine, $k_3$ is subparallel to (100), $k_1$ to [001], and $k_2$ to [010] . The hypersthene crystals consist of lamellae of othopyroxene and Ca-rich clinopyroxene, whereby $k_2$ and $k_3$ lie in the lamellae plane.

The ferrimagnetic component of the diopside crystal, which carries a significant ferrimagnetic AMS, shows no relationship to the mineral's crystallographic axes (Table S3, Fig. 3b, c). The augite crystals, on the other hand, have a large part of their high-field AMS arising from ferrimagnetic exsolutions in the crystal. There is good grouping of $k_3$ along the [010] axis of the crystal; $k_1$ and $k_2$ are also well grouped and lie in a plane containing the [100] and [001] crystallographic axes. The hypersthene crystal $k_1$ normal to the lamellae of the ortho- and clinopyroxene (Fig. 3c, d). The degree of ferrimagnetic anisotropy is highest in the pyroxenes, compared to the other crystal groups.

**Amphibole Crystals**

A study of the paramagnetic AMS for 28 single crystals was made by Biedermann et al. (2015a). Only five crystals showed a significant component of ferrimagnetic anisotropy, one actinolite crystal (Akt1) and four hornblende samples (Amph, Amph3, NMB535 and Hbl1). From these crystals three acquired a measurable IRM (Fig. 4a). After a rapid acquisition in low fields the IRM shows a more gradual approach to saturation in comparison with other minerals. $B_{CR}$ is relatively high, ranging from 40 mT for Amph1 to 110 mT for Akt1, which suggests the presence of a higher coercivity phase. Amph 3 also showed two sextets in Mössbauer spectroscopy, indicative of non-stoichiometric magnetite (cf. Biedermann et al. 2015a).

The principal axes of the paramagnetic AMS are related to the crystallographic axes of the crystral structure. For tremolite, actinolite and hornblende the paramagnetic $k_3$ is sub-parallel to (100) crystallographic axis, and $k_1$ is generally along [010]. Richterite has $k_2$ along [010] and $k_1$ and $k_3$ in a plane containing [100] and [001], whereas gedrite, which was the only orthoamphibole measured, has $k_3$ along [100] and $k_1$ along [001].

The ferrimagnetic component to the AMS is between 8% to 13% in all crystals except Amph3 in which it contributes 85% to the total high-field AMS (Table S4). The directions do not display a close relationship to the crystallographic axes of the crystals, however, $k_3$ lies generally within 20° from the plane that contains the normal to (100) and the [010] direction (Figure 4b, c). The ferrimagnetic ellipsoids are all neutral in shape and the degree of anisotropy, as reflected by k', is low except for NMB535.

**Feldspar Crystals**

Biedermann et al. (2016) reported on the AMS of 31 feldspar crystals with varying composition. Only eight samples possessed a significant ferrimagnetic anisotropy. These include

two amazonite, three orthoclase, one andesine and two sunstone crystals. The sunstone crystals contain visible, micron-sized laths of an opaque and red mineral (Fig. 5a). Two types of behaviour were found in the acquisition of IRM (Fig. 5b). One of the orthoclase and the two sunstone crystals show a rapid increase in the IRM in low fields and approach, but do not reach, saturation by 300 mT. $B_{CR}$ is between 19 mT to 40 mT. This indicates that the samples contain both low and high coercivity phases, which is further confirmed from a wasp-waisted hysteresis loop (Fig. 5 in Biedermann et al. 2016). Another orthoclase crystal and an amazonite crystal display a slower acquisition of IRM that is not saturated by 2000 mT. $B_{CR}$ between 300 mT and 560 mT indicates the dominance of a high coercivity phase that is most likely hematite.

Although the high-field AMS is very weak in all crystals, the anisotropy arising from the diamagnetic susceptibility shows a relationship to the samples crystallographic axes, with the most negative susceptibility close to [010] and the least negative susceptibility along [001]. The ferrimagnetic anisotropy of the alkali feldspar crystals does not display a strong relationship to the crystallographic axes of the minerals (Fig. 5 c, d, Table S5). The $k_2$ axes lie close to (100) for some crystals but the degree of anisotropy is extremely low. The $k_1$ axes for the sunstone crystals, however, are along the lath direction of the ferrimagnetic exolution, which is sub-parallel to [010] (Fig. 5 e). The shape of the ferrimagnetic ellipsoid is very variable from oblate to prolate for the feldspar crystals in general, and the degree of anisotropy is the weakest compared to all other mineral types.

**Carbonate Minerals**

A systematic study of the magnetic anisotropy in carbonate minerals was carried out by Schmidt et al. (2006) on calcite and Schmidt et al. (2007a) on other carbonate minerals. Only six

of nineteen calcite crystals and four of 19 carbonate crystals, including one cerrusite, one dolomite, one magnesite and one rhodochrosite crystal possessed a ferrimagnetic anisotropy. Because the carbonate minerals were not oriented with respect to crystallographic axes, only the calcite crystals will be discussed. The contribution of the ferromagnetic component to the total high-field AMS is low for all crystals (Table S6).

IRM is acquired rapidly in low fields in most crystals (Fig. 6a). Some crystals are saturated in fields below 300 mT, whereas other crystals are not saturated at the highest applied field. $B_{CR}$ ranges between 35 and 100 mT in general. C2 is an exception with a more gradual acquisition of IRM and a $B_{CR}$ around 600 mT (not shown). This suggests that the crystals contain a mixture of low coercivity minerals, e.g., magnetite and/or maghemite, and high coercivity minerals , most likely hematite.

Schmidt et al. (2006) demonstrated that the magnetic anisotropy of the non-ferrimagnetic susceptibility in the calcite crystals may be due to diamagnetism in the case that the iron content is < 400 ppm at room temperature, or paramagnetic anisotropy for higher iron concentration. For the diamagnetic anisotropy $k_3$ (most negative susceptibility) is along the [001] axis of the crystals, and for paramagnetic crystals $k_1$ is along the [001] crystallographic axis.

The ferrimagnetic anisotropy has a loose group of $k_1$ or $k_2$ towards 35° and tilted about 15° form the (001) plane (Fig. 6b). The $k_3$ and either $k_1$ or $k_2$ form a girdle about this direction. This grouping is close to a cleavage plane within the crystal, which suggests that the orientation of the ferrimagnetic phases is constrained by the cleavage plane, possibly as a consequence of epitaxial growth, or growth along a crack in the crystal (Fig. 6c). The shape of the ferrimagnetic ellipsoid is generally oblate, although C4A is strongly prolate. The degree of anisotropy is relatively high compared to other crystal groups. It is more similar to augite crystals, thus reflecting control of the

orientation of ferrimagnetic grains by the crystal structure, which gives it a higher degree of alignment.

## Discussion and Conclusions

Many crystals contain ferromagnetic (s.l.) exsolutions or inclusions. David Strangway's (1960) idea that ferrimagnetic minerals can reside as exsolutions within silicate minerals has been shown to be possible in many common rock-forming minerals (e.g., Bono and Tarduno, 2015; Feinberg et al., 2005; Palmer and Carmichael, 1973; Selkin et al., 2000; Smirnov et al., 2003; Usui et al., 2015; Wu et al., 1974). Inclusions are generally randomly oriented within the crystal, which means that they should not contribute strongly to any magnetic anisotropy of the crystal. Exsolutions, however, will be controlled by the crystal structure, such as cleavage or lattice planes, which will lead to a preferential alignment with respect to the host silicate. This is the case for clinopyroxene and the hypersthene crystals, in which the ferromagnetic (s.l.) contribution to the total AMS can be dominant. Preferentially oriented ferromagnetic exsolutions in pyroxenes have already been described in a number of studies (e.g., Bown and Gay, 1959; Doukhan et al., 1990; Feinberg et al., 2004; Fleet et al., 1980). The degree of this ferrimagnetic anisotropy, although weaker than what is found in a rock with texture, is relatively strong, and can contribute to the total anisotropy of the rock if the silicate crystals have a crystallographic preferred orientation. The phyllosilicate minerals have a strong cleavage related to their sheet structure, but the ferrimagnetic $k_1$ axes are tilted away from the normal to sheet structure and may reflect the stacking of the sheets. Therefore, the ferrimagnetic minerals may show an epitaxial control in growth. The other mineral whose ferromagnetic (s.l.) anisotropy is related to crystal cleavage is calcite. Both hematite and magnetite have been found to grow both on the surface and within calcite crystals. A good example

of hematite growth on calcite was shown by Walker et al. (1981) in the Triassic Moenkopi Formation from the Colorado Plateau.

Oligoclase that contains exsolutions of hematite is known as sunstone. Oligoclase has a very good {001} cleavage but also good {010} cleavage. The crystals of sunstone used in this study contained both magnetite and hematite, whereby the magnetite dominated the mineral's bulk magnetic properties. The ferrimagnetic fabric is dominated by laths of magnetite that are exsolved in the crystal cleavage and favor (010). The amazonite crystals and Orth1 have $k_3$ close to [010] but the degree of ferrimagnetic anisotropy is very weak.

The $k_1$ and $k_3$ axes in the olivine crystals lie approximately at 45° from [001] in general, even though the ferromagnetic (s.l.) contribution to the high-field AMS is usually < 10%. Biedermann et al. (2014b) speculated that there may be a mechanism that favors growth of inclusion in these directions, similar to what has been reported for Fe-Ni globules in chondritic olivine (Biedermann et al. 2014b). Further work, however, would be needed to understand this crystallographic relationship.

Most amphibole crystals did not contain a significant ferrimagnetic anisotropy, although it was clear that there were ferromagnetic (s.l.) inclusions in the crystals, based on their bulk susceptibility. Only five crystals possessed a ferrimagnetic anisotropy and these did not show any preference in the orientation of their principal axes.

The results from this study suggest that a preferred orientation of clinopyroxene, phyllosilicate and calcite minerals could lead to a preferential orientation of the ferromagnetic (s.l.) minerals in the rock if they occur as exsolutions within these minerals. The host phases can have a preferential orientation either due to emplacement of a magmatic body in the case of pyroxene, or sedimentary compaction in the case of phyllosilicate. Calcite alignment occurs usually due to

deformation, which would also affect the other minerals. If the ferromagnetic (s.l.) exsolutions lie in a preferred plane, then their remanent magnetization may be biased form the Earth's magnetic field direction towards the direction of their statistically aligned easy axis of magnetization. This would then give a paleomagnetic direction that does not reflect the latitude in which a rock formed or acquired its magnetization, and would also affect the intensity of magnetization Normally, mineral alignment is not so strong as to influence the remanent magnetization of a rock as a whole, especially if other ferromagnetic (s.l.) phases are present in the rock, e.g. as individual grains. A more serious problem can occur if single crystals are being used for determination of the paleointensity of the Earth's magnetic field (cf., Selkin et al., 2000). In this case, a preferential alignment of ferromagnetic (s.l.) exsolutions would mean that the field intensity would be dependent on the direction of the ambient field with respect to a preferential orientation of the easy axes of the ferromagnetic (s.l.) phase. For this reason, it is important that any crystal that is used for paleointensity determination should be screened for any ferromagnetic (s.l.) anisotropy.

Strangway correctly identified ferromagnetic inclusions and exsolutions within silicates as primary remanence carriers in igneous rocks (Strangway 1960). In addition to their size (single domain range), they also have the advantage compared to individual ferromagnetic (s.l.) grains that they are protected against alteration by their host silicate. If the crystallographic lattices of silicate minerals are randomly oriented, then ferrimagnetic inclusions can be faithful recorders of the Earth's magnetic field. Problems may arise, however, when oriented exsolutions in oriented silicates are the sole remanence carriers of a rock; their anisotropy may affect the direction and intensity of magnetization. In conclusion, a better understanding of the magnetic anisotropy of ferromagnetic (s.l.) exsolutions in particular in pyroxene, phyllosilicates, some feldspars and to a lesser extend in olivine, will help make paleomagnetic studies on single crystals more robust.

## Acknowledgements

We thank A. Kontny and J. Taruduno for their thoughtful comments for improving the manuscript. We kindly acknowledge P. Brack, M. Schmidt, H. Mattsson, and S.A. Bosshard (ETH-Zürich), A. Puschnig (Natura History Museum Basel) and A. Stucki (Siber + Siber, Aathal) for providing crystals. Results from this study were supported by the Swiss National Science Foundation (SNSF) under Projects: 21-50639.97, 200020-100224, 20020-143438, and 200021-129806. A.R.B. was supported by SNSF Project 167609.

## References

Bergmüller, F., Bärlocher, C., Geyer, B., Grieder, M., Heller, F., and Zweifel, P. 1994. A torque magnetometer for measurements of the high-field anisotropy of rocks and crystals. Meas. Sci. Technol. **5**: 1466-1470.

Biedermann, A.R., Koch, C.B., Lorenz, W.E.A., and Hirt, A.M. 2014a. Low-temperature magnetic anisotropy in micas and chlorite. Tectonophysics **629**: 63-74. doi: 10.1016/j.tecto.2014.01.015.

Biedermann, A.R., Koch, C.B., Pettke, T., and Hirt, A.M. 2015a. Magnetic anisotropy in natural amphibole crystals. American Mineralogist **100**(8-9): 1940-1951. doi: 10.2138/am-2015-5173.

Biedermann, A.R., Pettke, T., Angel, R.J., and Hirt, A.M. 2016. Anisotropy of magnetic susceptibility in alkali feldspar and plagioclase. Geophysical Journal International **205**(1): 479-489. doi: 10.1093/gji/ggw042.

Biedermann, A.R., Pettke, T., Koch, C.B., and Hirt, A.M. 2015b. Magnetic anisotropy in clinopyroxene and orthopyroxene single crystals. Journal of Geophysical Research-Solid Earth **120**(3): 1431-1451. doi: 10.1002/2014jb011678.

Biedermann, A.R., Pettke, T., Reusser, E., and Hirt, A.M. 2014b. Anisotropy of magnetic susceptibility in natural olivine single crystals. Geochemistry Geophysics Geosystems **15**(7): 3051-3065. doi: 10.1002/2014gc005386.

Bono, R.K., and Tarduno, J.A. 2015, Stable Earth, reversing field in the Ediacaran: A single crystal crystal stduy of the ca. 565 Ma Sept-iles Intrusive Suite in Laurentia. Geology **43**(2): 131-134.

Bown, M. G., and Gay, P. 1959. The identification of oriented inclusions in pyroxene crystals. American Mineralogist **44**(5-6): 592-602.

Buchan, K.L. 1979. Paleomagnetic studies of bulk mineral separates from the Bark Lake diorite, Ontario. Canadian Journal of Earth Sciences **16**(8): 1558-1565. doi: 10.1139/e79-142.

Buddington, A.F., and Lindsley, D.H. 1964. Iron-titanium oxide minerals and synthetic equivalents. Journal of Petrology **5**(2): 310-357. doi: 10.1093/petrology/5.2.310.

Carmichael, I.S.E., and Nicholls, J. 1967. Iron-titanium oxides and oxygen fugacities in volcanic rocks. Journal of Geophysical Research **72**: 4665–4687.

Cottrell, R: and Tarduno, J.A. 1999. Geomagnetic paleointneisty derived from single plagioclase crystals. Earth and Planetary Science Letters **169**: 1-5.

Doukhan, N., Ingrin, J., Doukhan, J.C. and Latrous, K. 1990. Coprecipitation of magnetite and amphibole in black star diopside: A 474 TEM study. American Mineralogist **75**(7-8): 840-846.

Dunlop, D.J., Ozdemir, O., and Rancourt, D.G. 2006. Magnetism of biotite crystals. Earth And Planetary Science Letters **243**(3-4): 805-819.

Feinberg, J.M., Wenk, H.R., Renne, P.R., and Scott, G.R. 2004. Epitaxial relationships of clinopyroxene-hosted magnetite determined using electron backscatter diffraction (EBSD) technique. American Mineralogist **89**(2-3): 462-466.

Feinberg, J.M., Scott, G.R., Renne, P.R., and Wenk, H.-R. 2005 Exsolved magnetite inclusions in silicates: Features determining their remanence behavior. Geology **33**(6): 513-516. doi: 10.1130/g21290.1.

Fleet, M.E., Wilcox, G.A., and Barnett, R.L. 1980. Oriented magnetite inclusions in pyroxene from the Grenville Province. Canadian Mineralogist **18**: 89-99.

Hargraves, R.B., and Young, W.M. 1969. Source of stable remanent magnetism in Lambertville diabase. American Journal of Science **267**: 1161–1177.

Jelinek, V. 1981. Characterization of the magnetic fabric of rocks. Tectonophysics **79**: T63-T67.

Jelínek, V. 1984. On a mixed quadratic invariant of the magnetic susceptibility tensor. Journal of Geophysics **56**: 58-60.

Lappe, S.-C., Church, N.S., Kasama, T., Bastos da Silva Fanta, B., Bromiley, G., Dunin-Burkowski, R.E., Feinberg, J.M., Russell, S., and Harrison, R.J. 2011. 2011 Mineral magnetism of dusty olivine: A credible recorder of pre-accretionary remanence. Geochemistry, Geophysics, Geosystems **12**: Q12Z35. doi: 10.1029/2011GC003811.

Larson, E., Ozima, M., Nagata, T., and Strangway, D. 1969. Stability of remanent magnetisation of igneous rocks. Geophysical Journal of the Royal Astronomical Society **17**(3): 263-292. doi: 10.1111/j.1365-246X.1969.tb00237.x.

Leroux, H.G., Libourel, L., Lamella, L., and Guyot, F. 2003. Experimental study and TEM characterization of dusty olivine in chondrites: Evidence for formation by in situ reduction. Meteoritics and Planetary Science **38**: 81-94. doi: 10.1111/j.1945-5100.2003.tb01047.x.

Martín-Hernández, F., and Hirt, AM. 2001. Separation of ferrimagnetic and paramagnetic anisotropies using a high-field torsion magnetometer. Tectonophysics **337**(3-4): 209-221. doi: 10.1016/S0040-1951(01)00116-0.

Martín-Hernández, F., and Hirt, A. 2003. The anisotropy of magnetic susceptibility in biotite, muscovite and chlorite single crystals. Tectonophysics **367**(1-2): 13-28. doi: 10.1016/S0040-1951(03)00127-6.

Martin-Hernandez, F., and Hirt, A.M. 2004. A method for the separation of paramagnetic, ferrimagnetic and haematite magnetic subfabrics using high-field torque magnetometry. Geophysical Journal International **157**(1): 117-127. doi: 10.1111/j.1365-246X.2004.02225.x.

Palmer, H.C., and Carmichael, C.M., 1973. Paleomagnetism of some Grenville Province rocks, Canadian Journal of Earth Sciences **10**(8): 1175-1190.

Schmidt, V., Gunther, D., and Hirt, A. 2006. Magnetic anisotropy of calcite at room-temperature. Tectonophysics **418**(1-2): 63-73. doi: 10.1016/j.tecto.2005.12.019.

435 Schmidt, V., Hirt, A.M., Hametner, K., and Gunther, D. 2007a. Magnetic anisotropy of carbonate
436 minerals at room temperature and 77 K. American Mineralogist **92**(10): 1673-1684. doi:
437 10.2138/am.2007.2569.
438 Schmidt, V., Hirt, A.M., Rosselli, P., and Martin-Hernandez, F. 2007b. Separation of diamagnetic
439 and paramagnetic anisotropy by high-field, low-temperature torque measurements.
440 Geophysical Journal International **168**(1): 40-47. doi: 10.1111/j.1365-246X.2006.03202.x.
441 Selkin, P.A., Gee, J.S., Tauxe, L., Meurer, W.P., and Newell, A.J. 2000. The effect of remanence
442 anisotropy on paleointensity estimates: a case study from the Archean Stillwater Complex.
443 Earth and Planetary Science Letters **183**(3-4): 403-416.
444 Smirnov, A.V., Tarduno, J.A., and Pisakin, B.N. 2003. Paleointensity of the early geodynamo
445 (2.45 Ga) as recorded in Karelia: A single crystal approach. Geology **31** (5): 415-418.
446 Strangway, D.W. 1960. Magnetic studies of some diabase dikes. Journal of Geophysical Research
447 **65**(8): 2526-2526.
448 Strangway, D.W., Larson, E.E., and Goldstein, M. 1968. A possible cause of high magnetic
449 stability in volcanic rocks. Journal of Geophysical Research **73**(12): 3787-3795. doi:
450 10.1029/JB073i012p03787.
451 Tarduno, J.A., Cottrell, R.D., and Smirnov, A.V. 2006. The paleomagnetism of single silicate
452 crystals: Recording geomagnetic field strength during mixed polarity intervals, superchrons,
453 and inner core growth. Reviews Of Geophysics **44**(1).
454 Usui, Y., Shiuya, T., Sawaki, Y., and Komiya, T. 2015. Rock magnetism of tiny exsolved
455 magnetite in palgioclase. from a Paleoarchean granitoid in the Pilbara craton. Geochemistry
456 Geophysics Geosystems **16** (1): 112-115. doi: 10.1002/2014GC005508.
457 Wu, Y.T., Fuller, M.D., and Schmidt, V.A. 1974. Microanalysis of NRM in a granodiorite
458 intrusion. Earth and Planetary Science Letters **23**: 275–285.
459

Figure Captions

Figure 1. a) Acquisition of IRM for selected crystals of phyllosilicate minerals; b) orientation of the principal axes of the ferrimagnetic AMS for phyllosilicate crystals; and c) schematic illustration of the crystal structure and preferred directions in which principal axes of the ferrimagnetic AMS lie. All directions are shown on lower hemisphere, equal-area projection with $k_1$ represented by squares, $k_2$ by triangles, and $k_3$ by circles in this and subsequent figures. Light grey planes or cones indicate preferred direction of the principal axes of the ferrimagnetic AMS, in this and subsequent figures.

Figure 2. a) Acquisition of IRM for selected crystals of olivine; b) orientation of the principal axes of the ferrimagnetic AMS (adapted from Biedermann et al., 2014b); and c) schematic illustration of the crystal structure and preferred directions of the principal axes of the ferrimagnetic AMS.

Figure 3. a) Acquisition of IRM for selected crystals of pyroxene; b) orientation of the principal axes of the ferrimagnetic AMS for clinopyroxene (adapted from Biedermann et al., 2015b); c) schematic illustration of the crystal structure and preferred directions of the principal axes of the ferrimagnetic AMS for clinopyroxene and hypersthene composed of lamellae of ortho- and clinopyroxene; and d) orientation of the principal axes of the ferrimagnetic AMS for hypersthene (adapted from Biedermann et al., 2015b).

Figure 4. a) Acquisition of IRM for selected crystals of amphibole; b) orientation of the principal axes of the ferrimagnetic AMS; and c) schematic illustration of the crystal structure.

Figure 5. a) Photomicrograph in plane light showing inclusions of magnetite/maghemite (black) and hematite (red) with direction of $k_1$; b) acquisition of IRM for selected crystals of feldspar; c) orientation of the principal axes of the ferrimagnetic AMS from alkali feldspar crystals; d) schematic illustration of the crystal structure and preferred directions of the principal axes of the ferrimagnetic AMS; and e) orientation of the principal axes of the ferrimagnetic AMS from plagioclase crystals.

Figure 6. a) Acquisition of IRM for selected crystals of carbonate minerals; b) orientation of the principal axes of the ferrimagnetic AMS in calcite; and c) schematic illustration of the calcite crystal structure, in which the dashed line indicates the crystallographic c-axis.

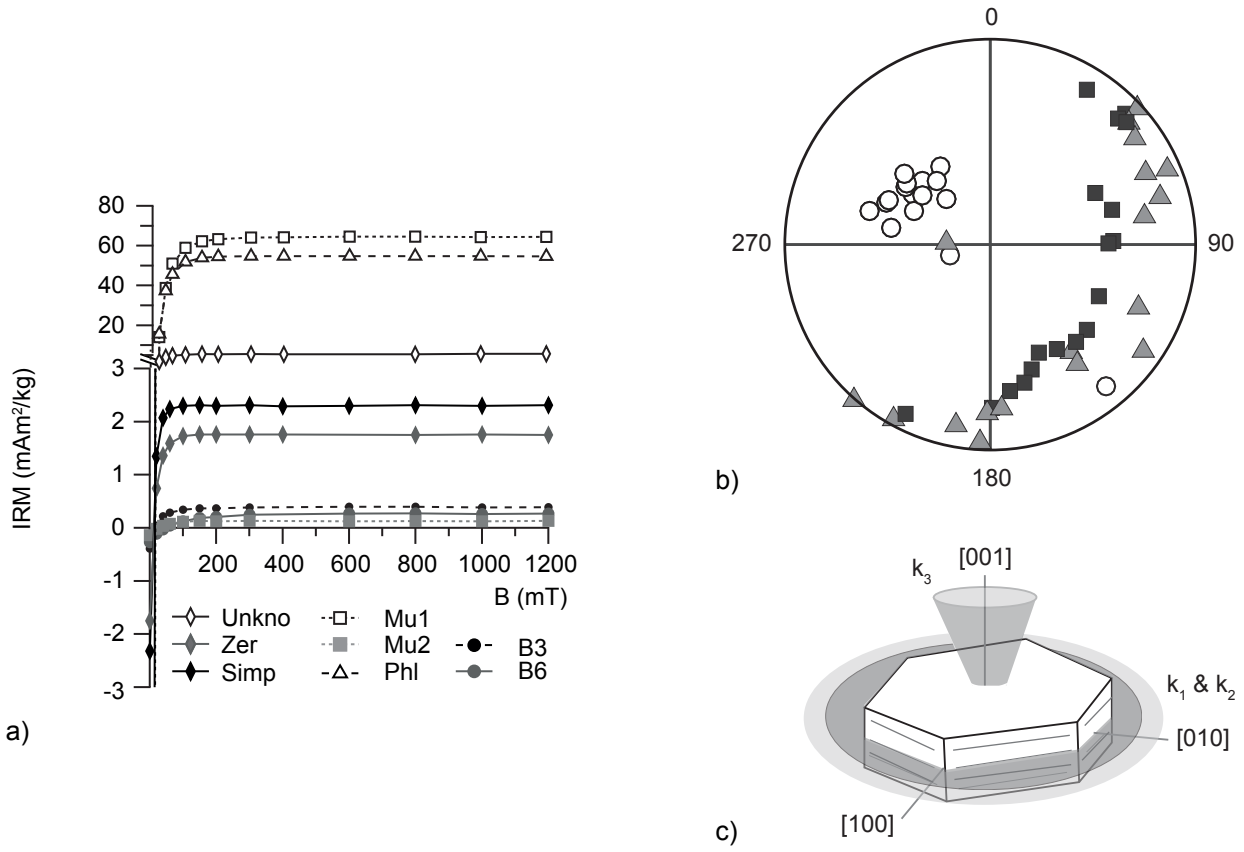


Figure 1. a) Acquisition of IRM for selected crystals of phyllosilicate minerals; b) orientation of the principal axes of the ferrimagnetic AMS for phyllosilicate crystals; and c) schematic illustration of the crystal structure and preferred directions in which principal axes of the ferrimagnetic AMS lie. All directions are shown on lower hemisphere, equal-area projection with k1 represented by squares, k2 by triangles, and k3 by circles in this and subsequent figures. Light grey planes or cones indicate preferred direction of the principal axes of the ferrimagnetic AMS, in this and subsequent figures.

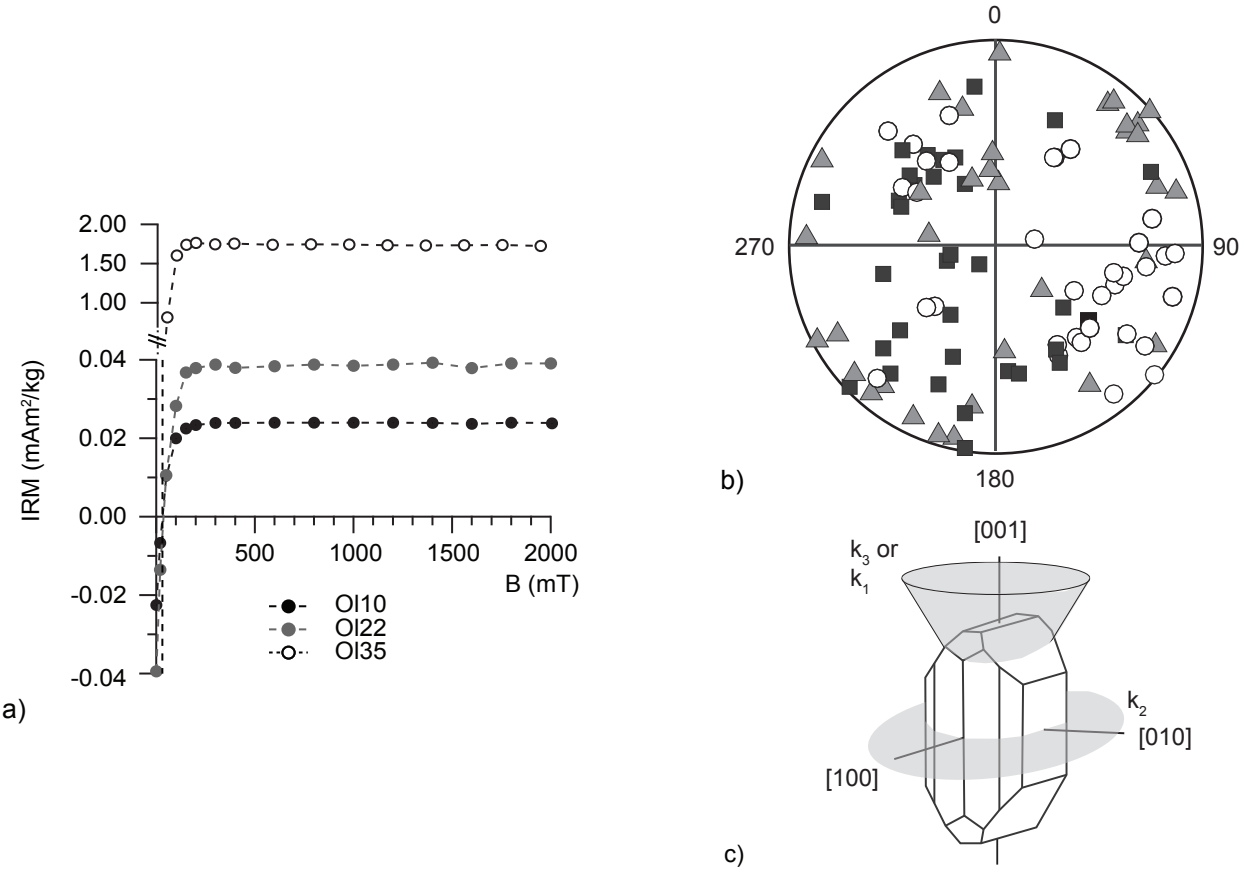


Figure 2. a) Acquisition of IRM for selected crystals of olivine; b) orientation of the principal axes of the ferrimagnetic AMS (adapted from Biedermann et al., 2014b); and c) schematic illustration of the crystal structure and preferred directions of the principal axes of the ferrimagnetic AMS.

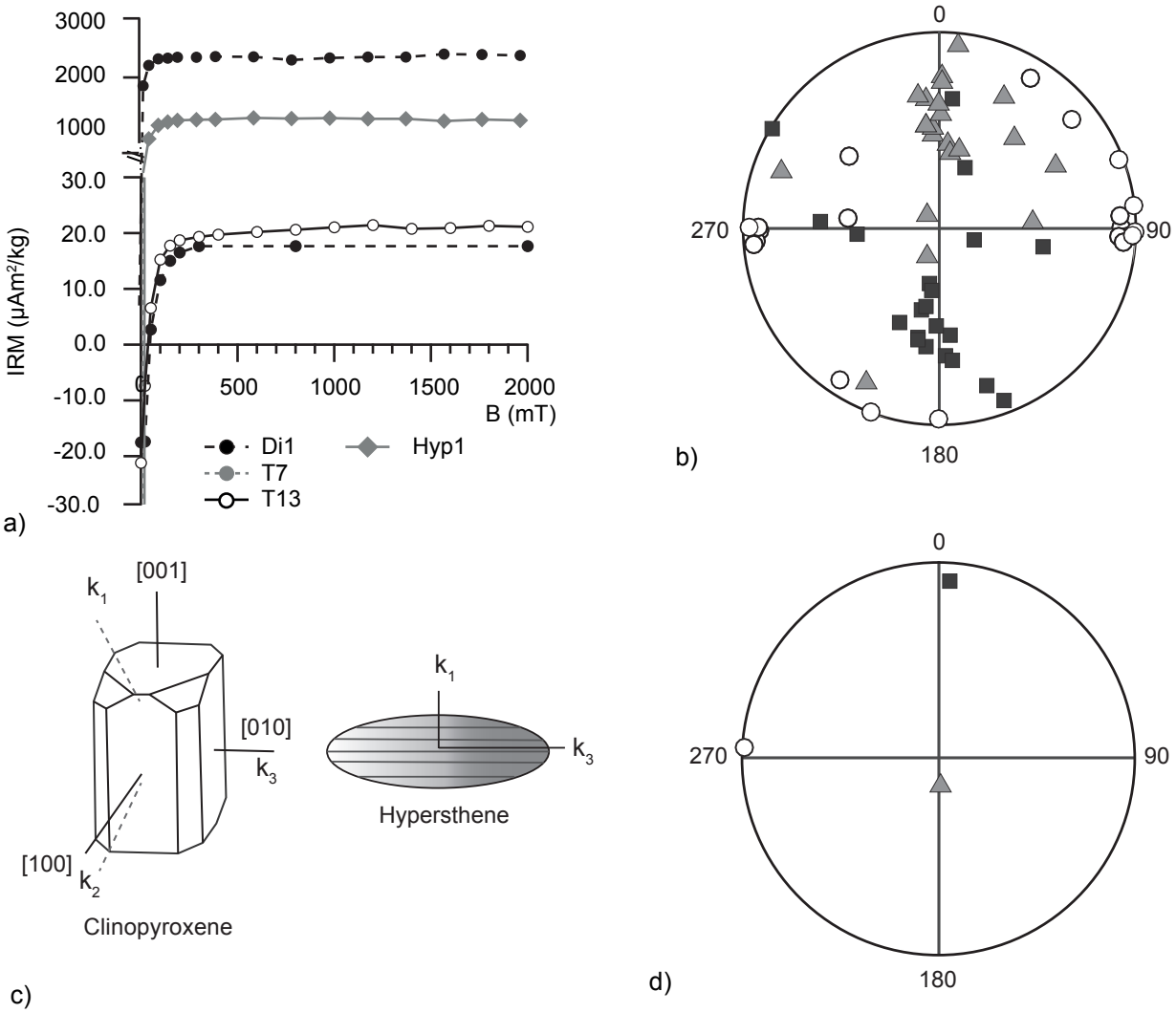


Figure 3. a) Acquisition of IRM for selected crystals of pyroxene; b) orientation of the principal axes of the ferrimagnetic AMS for clinopyroxene (adapted from Biedermann et al., 2015b); c) schematic illustration of the crystal structure and preferred directions of the principal axes of the ferrimagnetic AMS for clinopyroxene and hypersthene composed of lamellae of ortho- and clinopyroxene; and d) orientation of the principal axes of the ferrimagnetic AMS for hypersthene (adapted from Biedermann et al., 2015b).

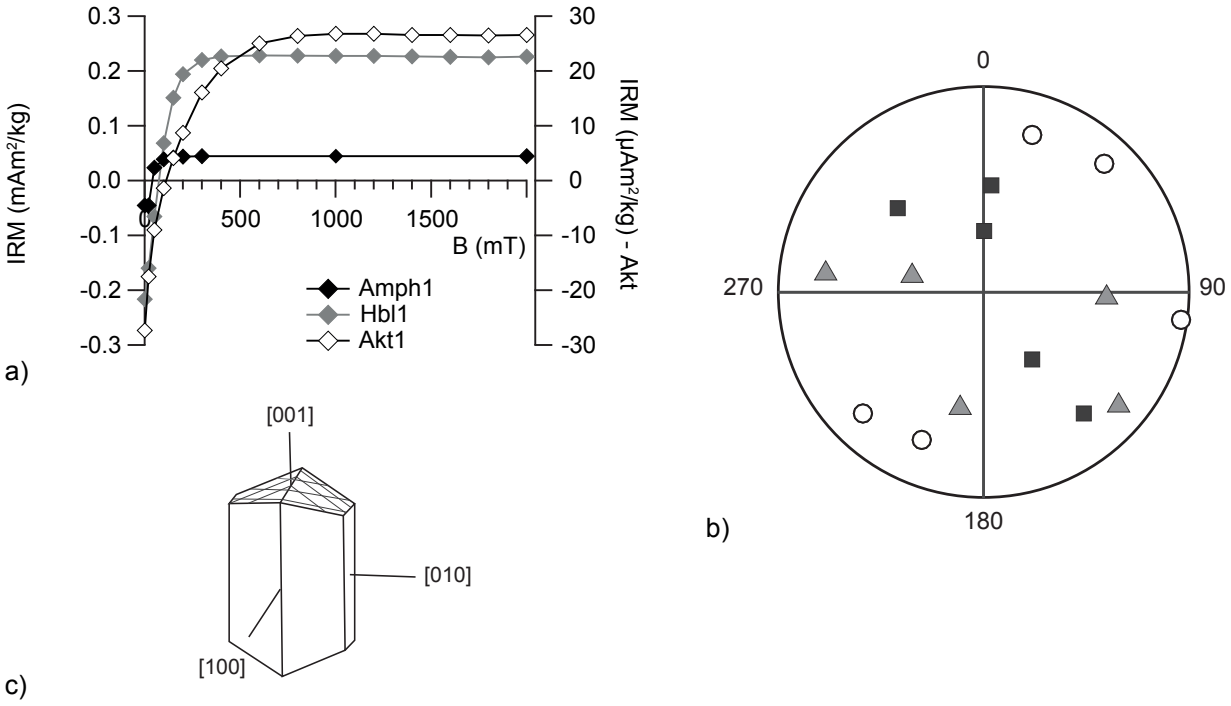


Figure 4. a) Acquisition of IRM for selected crystals of amphibole; b) orientation of the principal axes of the ferrimagnetic AMS; and c) schematic illustration of the crystal structure.

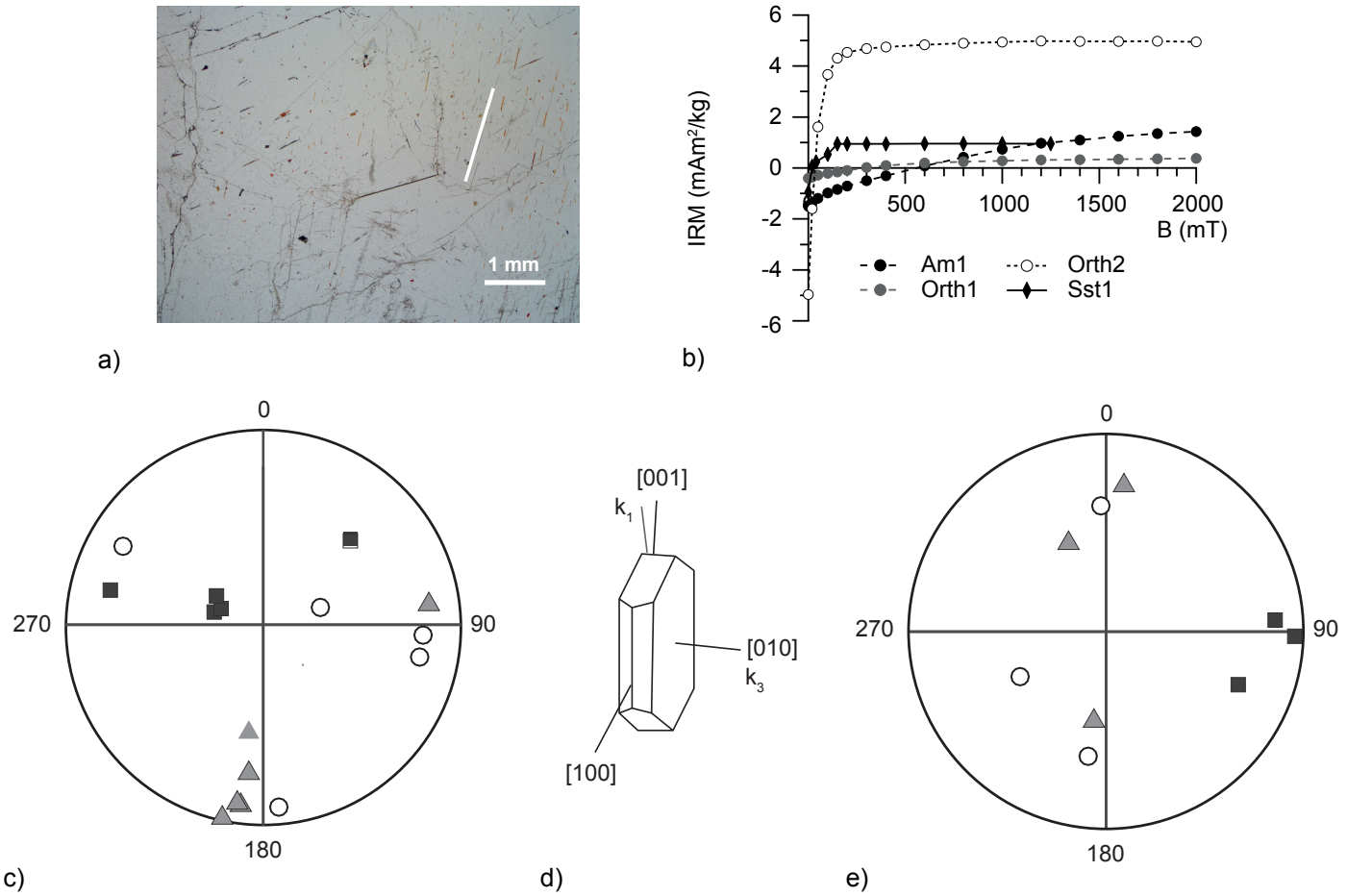


Figure 5. a) Photomicrograph in plane light showing inclusions of magnetite/maghemite (black) and hematite (red) with direction of k1; b) acquisition of IRM for selected crystals of feldspar; c) orientation of the principal axes of the ferrimagnetic AMS from alkali feldspar crystals; d) schematic illustration of the crystal structure and preferred directions of the principal axes of the ferrimagnetic AMS; and e) orientation of the principal axes of the ferrimagnetic AMS from plagioclase crystals.

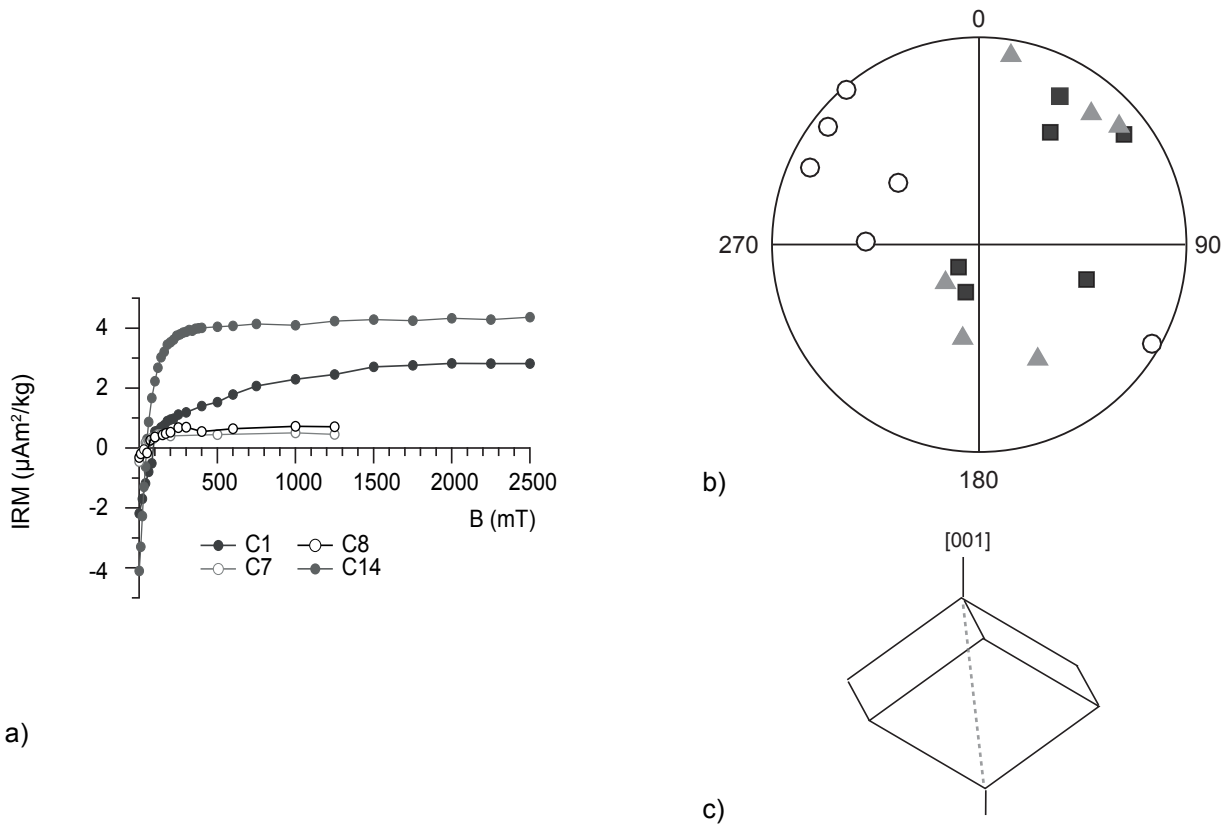


Figure 6. a) Acquisition of IRM for selected crystals of carbonate minerals; b) orientation of the principal axes of the ferrimagnetic AMS in calcite; and c) schematic illustration of the calcite crystal structure, in which the dashed line indicates the crystallographic c-axis.